

*Research*

Titanium Dioxide Substrates as Sensors for Detection of Platelets and Extracellular Particles from Blood Plasma

Rawat Niharika^{1,*}, Junkar Ita², Benčina Metka², Lampe Tomaž³, Kralj-Iglič Veronika³, Iglič Aleš¹

1. University of Ljubljana, Faculty of Electrical Engineering, Laboratory of Physics, Ljubljana, Slovenia
 2. Department of Surface Engineering, Jožef Stefan Institute, Ljubljana, Slovenia Nomadic College, Rome
 3. University of Ljubljana, Faculty of Health Sciences, Laboratory of Clinical Biophysics, Ljubljana, Slovenia
- * Correspondence: Niharika Rawat; niharika.rawat@fe.uni-lj.si

Citation: Rawat N, Junkar I, Benčina M, Kralj-Iglič V, Iglič A. Titanium Dioxide Substrates as Sensors for Detection of Platelets and Extracellular Particles from Blood Plasma Proceedings of Socratic Lectures. 2024, 11, 92-101.
<https://doi.org/10.55295/PSL.11.2024.11>

Publisher's Note: UL ZF stays neutral with regard to jurisdictional claims in published maps and institutional affiliations.



Copyright: © 2024 by the authors. Submitted for possible open access publication under the terms and conditions of the Creative Commons Attribution (CC BY) license (<https://creativecommons.org/licenses/by/4.0/>).

Abstract:

Biosensors are pivotal in biomedical applications, particularly for disease detection, diagnosis, treatment, health management, and monitoring. Titanium dioxide (TiO₂) is a prominent material for biosensors due to its biocompatibility, corrosion resistance, and availability in various nanostructured forms. This study explores the interaction of platelets and extracellular vesicles (EVs) with different TiO₂ surface morphologies using flow cytometry (FCM) and scanning electron microscopy (SEM). Blood plasma samples were incubated with various TiO₂ surfaces to evaluate particle counts and characteristics. FCM results indicated a higher abundance of platelets compared to EVs, with significant fragmentation observed post-centrifugation. SEM analysis confirmed platelet activation and fragmentation, with the microflowered TiO₂ surface displaying fewer vesicles due to its rough topography. The findings suggest that while TiO₂ surface structuring minimally impacts particle counts, it influences platelet and EV interactions, highlighting the need for advanced detection techniques and further investigation into surface interactions.

Keywords: cold gaseous plasma; atmospheric pressure plasma; plasma technology; dental medicine; extracellular vesicles, surface treatment

1. Introduction

Biosensors play a crucial role in the biomedical field, contributing to disease detection, treatment, diagnosis, health management, and monitoring. Biosensors hold a significant position in biomedical field since they provide early stage diagnostics of diseases, targeted drug delivery to diseased cells and nanorobots which are basically miniaturized biomedical devices. Titanium dioxide (TiO_2) is the most widely used metal oxide nanomaterial for biosensors, due to its advantageous properties such as bio inertness and resistance to corrosion in body fluids, making it suitable for various biological applications. The advancement of biosensors using nanomaterials has significantly facilitated the assessment of abnormalities in body fluids like blood, saliva, urine, and serum. These biosensors are particularly effective in detecting biomarkers, such as cells or mutated DNA, associated with tumorous or pre-tumorous tissues (Turner, 2013). In the fabrication of biosensors, nanoparticles are promising candidates as they can enhance sensitivity by improving system conductivity and amplifying signals providing more active sites for biological entities because of their high surface to volume ratio (Solanki et al., 2011). TiO_2 is chosen for its non-toxicity, biocompatibility, low cost, and good conductivity. A distinguishing feature of TiO_2 from other metal oxide nanomaterials is its availability in various morphologies, such as nanoparticles, nanorods, nanotubes, and nanobelts (**Figure 1**). For constructing a biosensor, a crucial step is a biomarker for specific condition or disease to detect these species from biofluids. This involves a microsystem where a bioreceptor (comprising of nucleic acids, membranes, enzymes, antibodies, extracellular vesicles (EVs), etc.) is connected to a transducing element. This transducer (which can be optical, electrochemical, magnetic, piezoelectric, micromechanical, or thermometric) produces, intercepts, and converts signals after the analyte attaches to the biosensor (Mavrič et al., 2018; Mittal et al., 2017). Biosensors are efficient in differentiating specific analytes, even at lower concentrations, offering easier data collection and interpretation for various applications.

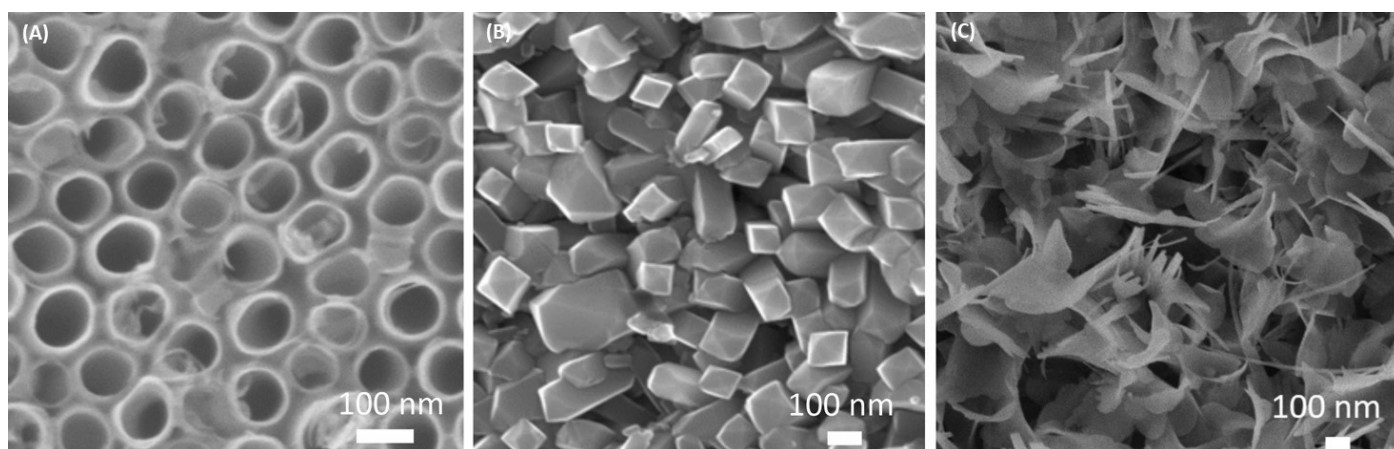


Figure 1. TiO_2 nano-structured surfaces a) nanotubes, b) nanocubes and c) nanoflakes.

Nanomaterials exhibit distinct physicochemical properties (such as solubility vapour, boiling point, pressure and reactivity) compared to their bulk counterparts, influenced by their high surface-to-volume ratio and quantum confinement effect (QCE). Their large surface energy, arising from more exposed atoms, makes nanomaterials particularly suitable for sensing technology. Since most structures, molecules and biological processes of human system occur at nanoscale ranges (eg. DNA has approximately 2 nm diameter) therefore nanomaterials are preferred in sensing technology. The absence of effective measures to control the coronavirus resulted in worldwide lockdowns, significantly impacting the global economy and leading to a standstill. Metal oxide nanostructures are used in various biosensor contexts, extending beyond the scope of the novel coronavirus disease (Covid-19) caused by severe acute respiratory syndrome coronavirus 2 (SARS-CoV-2). For this purpose, Vadlamani et al. (2020) developed an economical yet highly sensitive electrochemical sensor using cobalt-functionalized TiO_2 nanotubes (Co-TNTs) for the rapid detection of SARS-CoV-2. This sensor operates by sensing the spike protein, specifically the



receptor binding domain (RBD) of the virus. The synthesis of TNTs involved a conventional one-step anodization (Junkar et al., 2016; Kulkarni et al., 2015) setup, followed by cobalt functionalization using the incipient wetting method. The entire system was connected to a potentiostat for data collection. Remarkably, even at low concentrations ranging from 14 to 100 nanomolar (nM), the sensor successfully detected the S-RBD protein of SARS-CoV-2. Furthermore, the sensor exhibited a linear response in the detection of the viral protein at various concentrations. This underscores the effectiveness of the system in rapidly detecting SARS-CoV-2 S-RBD protein in approximately 30 seconds, making it suitable for point-of-care diagnostics using nasal secretions and saliva samples.

In the early stages of cancer detection using biosensors, the analysis of biomarkers in urine, blood, and body fluids is essential for oncology, aiding in cancer diagnosis and prognosis (Golubnitschaja and Flammer, 2007; Strimbu and Tavel, 2010). Cancer biomarkers are essentially proteins overexpressed in body fluids like blood or serum, originating from cancerous cells. Detecting these biomarkers during the initial phase of cancer is challenging due to their low concentrations (Wulfschuhle et al., 2003). For this purpose, extracellular vesicles (EVs) serve as ideal cancer biomarkers, offering a minimally invasive diagnostic method with added advantages for biosensors (Kralj-Iglič, 2015). EVs have diverse applications, including the diagnosis of bodily abnormalities and targeted drug delivery. TiO₂ nanoparticles have been investigated for a smart pH-responsive drug delivery system, where TiO₂ nanoparticles loaded with doxorubicin form a doxorubicin/TiO₂ nanocomposite for the treatment of solid tumors and hematological malignancies (H. Zhang, Wang, Chen, & Wang, 2012). TiO₂'s drug-eluting mechanism has also been applied in coronary stents (Junkar et al., 2016a) and orthopedic implants (Popat et al., 2007). Nanotubes, with their favorable transport pathways, enhanced substrate adhesion, and high surface area, present several advantages over different nanomaterial morphologies, making them well-suited for biosensing applications (Xiao et al., 2011). A sophisticated TiO₂ system, such as the TiO₂-NTs/CdS:Mn/CdTe sensor, has been investigated, with nanotubes acting as the base. This sensor is applicable for detecting MMP-2, whose overexpression is associated with various cancers and serves as the basis for biomarker-based expression techniques like ELISA, RIA, and IHC. The TiO₂-based system demonstrates definite electron transfer and inhibition of charge recombination, associated with a cascade effect of charge carriers. In this system, SiO₂ coated with MMP-2 antibodies was employed for signal amplification, resulting in a low detection limit of 3.6 fg/mL for MMP-2 detection (Fan et al., 2014).

The utilization of TiO₂ in sensors for the detection of platelets and extracellular particles from blood plasma represents a promising avenue in biomedical research and diagnostics. In the context of blood plasma analysis, the detection of platelets and extracellular particles is crucial for understanding various physiological and pathological conditions. Platelets play a key role in hemostasis, wound healing, and immune response, while extracellular particles, such as extracellular vesicles (EVs) (Božič et al., 2022; Romolo et al., 2022), carry valuable information about cellular activities and can serve as biomarkers for diseases. Liquid biopsies (Martín-Gracia et al., 2020) represent a highly promising alternative to traditional tissue biopsies for the detection of cancer, monitoring tumor progression, and tracking tumor evolution (Castro-Giner et al., 2018). Recently, tumor-derived extracellular vesicles (EVs) have emerged as an alternative source of biomarkers in liquid biopsies. Despite initially being considered cellular waste, it is now understood that EVs play a significant role in intercellular communication and are involved in various normal and pathological processes, including cancer (Cordonnier et al., 2017). The cargoes carried by EVs depend on their parent cells, making them promising prognostic elements (Zhang et al., 2019). However, the clinical translation of EVs has been hindered by the use of complex and time-consuming traditional methods for isolation and analysis (Dong et al., 2019). Additionally, the high heterogeneity of EV isolates, containing a mix of EVs from different origins, sizes, and cargo contents, poses a challenge for their characterization (Li et al., 2019; Lim et al., 2020). In this context, there is a need for new analytical platforms that can conduct high-throughput analyses in an easy and sensitive manner without requiring extensive sample pre-treatment. Ideally, point-of-care (POC) biosensors would enable the sensitive, selective, and rapid detection of EVs while being user-friendly and cost-effective. Although significant efforts have been invested in developing novel biosensors for EV



analysis based on microfluidics, nanomaterials, or plasmonics, the majority of these platforms are still at the proof-of-concept stage and have not yet entered the market. Therefore, extensive research on TiO₂-based sensors for the detection of platelets and extracellular particles from blood plasma needs to be done, as it would offer a sensitive, specific, and biocompatible platform for understanding and monitoring various physiological and pathological conditions.

2. Material and Methods

2.1. Blood sampling

Blood was donated by an author (a female with no record of disease). Collection was established in the morning after fasting for a minimum of 12 h overnight. A G21 needle (Micro lance, Becton Dickinson, Franklin Lakes, NJ, USA) and 2.7 mL evacuated tube with trisodium citrate (BD Vacutainers, 367714A, Becton Dickinson, Franklin Lakes, NJ, USA) were used. Blood was centrifuged at 300g and 18°C for 10 minutes. Supernatant (taken cca 5 mm above the haematocrit boundary) was diluted with phosphate and citrate buffered saline in proportion 1 to 8 to obtain plasma samples.

2.2. Preparation of microflowered TiO₂ substrates

Titanium foils, which were 0.10 mm thick and had a purity exceeding 99.6%, were utilized to manufacture nanostructures. Pre-anodization, the foils underwent cleaning via successive ultrasonication in acetone, ethanol, and deionized water for 5 minutes each, followed by drying in a nitrogen stream. Electrolytes consisting of ultra-pure deionized water, sodium chloride (NaCl) and ethylene glycol were used. The anodization experiments were conducted at room temperature under 60 volts for 1 hour, employing an atmospheric-pressure plasma jet (APPJ) as the cathode. Our custom-built APPJ setup comprised a tubular capillary (acting as a discharge microreactor) crafted from an insulating material like glass or quartz, several electrodes (one grounded and the other supplying power to the discharge), an RF step-up transformer, and an RF (375 kHz) power source. The grounded electrode was structured as a ring surrounding the glass tube near the gas outlet, while the powered electrode (a slender, lengthy metallic tube) was situated within the glass tube. A gas supply mechanism (comprising bottles and mass flow controllers) regulated the desired flow rates (up to 1000 sccm for helium or argon) within the discharge zone.

2.3. Preparation of plasma treated TiO₂ substrates

The untreated Ti foil underwent oxygen plasma treatment within a plasma reactor. The plasma was generated using an inductively coupled RF generator running at 13.56 MHz and delivering around 800 W of power. Oxygen from a commercial source was introduced into the discharge chamber, maintaining a constant pressure of 50 Pa, which allowed for the highest level of gaseous molecule dissociation as indicated by catalytic probes. The samples, positioned on a glass holder, underwent treatment for 10 seconds.

2.4. Incubation of plasma

Plasma samples were incubated in Eppendorf tubes alone or with an added mica plate at room temperature on Orbital shaker for 1 hour.

2.5. Interaction of plasma with titanium dioxide plates

Plates (plate size: approx. 5×5mm) were inserted into eppendorf tubes (1.5mL, polypropylene), 460 μL of the sample was added and incubated at room temperature on a mixer (orbital shaker, 250-300/min) for 1h. 20 μL was taken for FCM analysis. Then, the samples were centrifuged for 20 min at 5000g and 4°C in the Centric 200R centrifuge with Lilliput rotor (Domel, Železniki, Slovenia). The supernatant (430 μL) and the pellet (30 μL) were pipetted off and the plate was prepared for scanning electron microscopy (SEM).

2.6. Flow cytometry of samples

The particle numbers in samples from plasma were estimated by flow cytometry using a MACSQuant Analyzer flow cytometer (Miltenyi Biotec, Bergisch Gladbach, Germany) and the related software. The following instrument settings were employed: CV settings: FSC: 458 V; SSC: 467 V with a trigger set to 1.48; B3: 300 V; and R1: 360 V. Particles were detected



from the forward (FSC) and side scatter parameters (SSC). Samples were mixed by pipetting before measurement, and 20,000 events per well were acquired. Data were analyzed using Aurora software or FlowJo software (BD Biosciences, Franklin Lakes, NJ, USA). The gates defining regions in the scatterplots pertaining to the populations of particles (P2*, and Pa*) were set in a preliminary study on the basis of experience with previously analyzed several blood samples (Božič et al., 2022). The P2* gate pertains mostly to platelets and the Pa* gate pertains to sub-cellular sized particles. The regions in the smaller scale settings were set by the shape of the event clouds.

2.7. Scanning Electron Microscopy

The samples were fixed with OsO₄ as adapted from [48]. Samples were imaged on titanium/mica plates. The plates were incubated in 39.3 mM double distilled water solution of OsO₄ for 2 h. Then they were washed 3 times with distilled water (10 min each), dehydrated in graded series of ethanol (30%, 50%, 70%, 80%, 90%) and absolute ethanol, each step 10 min. Absolute ethanol was replaced twice. Then they were washed in hexamethyldisilazane (mixed with absolute ethanol; 30% and 50%) and in absolute hexamethyldisilazane, each step 10 min. The samples were left to dry in air overnight. For examination under JSM-6500F Field Emission Scanning Electron Microscope (JEOL Ltd., Tokyo, Japan), the samples were sputtered with Au/Pd (PECS Gatan 682).

3. Results and Discussion

Table 1 shows flow cytometric count (Jeran et al., 2023) of P2* and Pa* particles in the samples. The P2* particles were considerably more numerous than the Pa* particles, in particular in the samples that underwent incubation and in the pellet after centrifugation. Comparing the incubated samples with the centrifuged ones it can be seen that centrifugation depleted the samples of P2* particles while some increase of the Pa* particles was observed in the pellet after centrifugation. This can be interpreted by destruction of platelets during centrifugation resulting in fragments that were then detected within the Pa* gate. However, the majority of EVs is expected to be smaller than the threshold limit of the FCM and were therefore not detected. It can be seen that the surface structuring of TiO₂ did not have a notable effect on the count of both types of particles, however, mica seems to have destructed platelets more effectively than TiO₂.

Table1. Flow cytometry count of P2* and Pa* particles in diluted plasma (PVRP) samples treated by incubation or centrifugation.

	Incubation		Supernatant after centrifugation		Pellet after centrifugation	
	P2* (10 ⁶ /mL)	Pa* (10 ⁶ /mL)	P2* (10 ⁶ /mL)	Pa* (10 ⁶ /mL)	P2* (10 ⁶ /mL)	Pa* (10 ⁶ /mL)
PRP	52.99	0.92	0.18	0.06	32.70	1.44
PRP+EV	54.96	1.05	0.23	0.55	31.79	1.52
PRP on Ti foil	53.71	0.96	0.23	0.05	34.24	1.56
PRP+EV on Ti foil	55.30	1.06	0.51	0.48	29.84	1.48
PRP on Flowers_TiO ₂	52.91	1.04	0.35	0.07	33.50	1.47
PRP+EV on Flowers_TiO ₂	57.63	1.28	0.25	0.53	34.45	1.57
PRP on P_TiO ₂	52.99	0.91	0.28	0.06	30.43	1.43
PRP+EV on P_TiO ₂	55.15	1.08	0.50	0.50	31.97	1.51

P2* corresponds mainly to platelets, in case of fragmentation of erythrocytes and leukocytes also larger microvesicles; the Pa* population contains EVs, lipoproteins, and other submicron particles.

Based on the results of the analysis of blind samples (without foil), there was no apparent binding of particles to any of the surfaces. In all samples, after centrifugation, we measured a total of more particles in the P2* regions than in the blind sample, except in the case of mica, where the result of this measurement was unreliable due to plate fragmentation and removal of part of the pellet with it. According to the results of flow cytometry (FCM) after incubation (with mixing), it appears that 5-30% additional EVs were formed in samples with microstructured Ti and mica, while untreated and nanostructured were not significantly different from the blind. After centrifugation, generally in the supernatants of the test samples (with Ti plates), there were more platelets (on average +70%) and fewer EVs (on average -7%) than in the blind sample. Differences between pellets were minimal, <10%, and trends in comparing PRP and PRP+EV were often inconsistent (reversed), making it very difficult to draw any conclusions. So, this time we rely entirely on SEM analysis; because we detect EVs less reliably with flow cytometry, it will be interesting to see if they have bound better to any surfaces. Several factors could contribute to the "poor" binding in this experiment - the high position of the foil in the microcentrifuge, higher dilution with buffer (impact on interactions).

Figure 2 shows samples containing platelets and EVs on untreated Ti foil (Ti foil) as imaged with SEM. It can be seen that the platelets (indicated by black arrows in Figure 2B and 2D) are highly activated exhibiting tubular protrusions. It can therefore be expected that the shed fragments and remnants of the cells contribute to the Pa* count by FCM. In Figures 2A and 2B numerous dendritic and extended platelets along with numerous vesicles can be observed whereas in case of Ti_PRP+EV only occasional vesicles were observed.

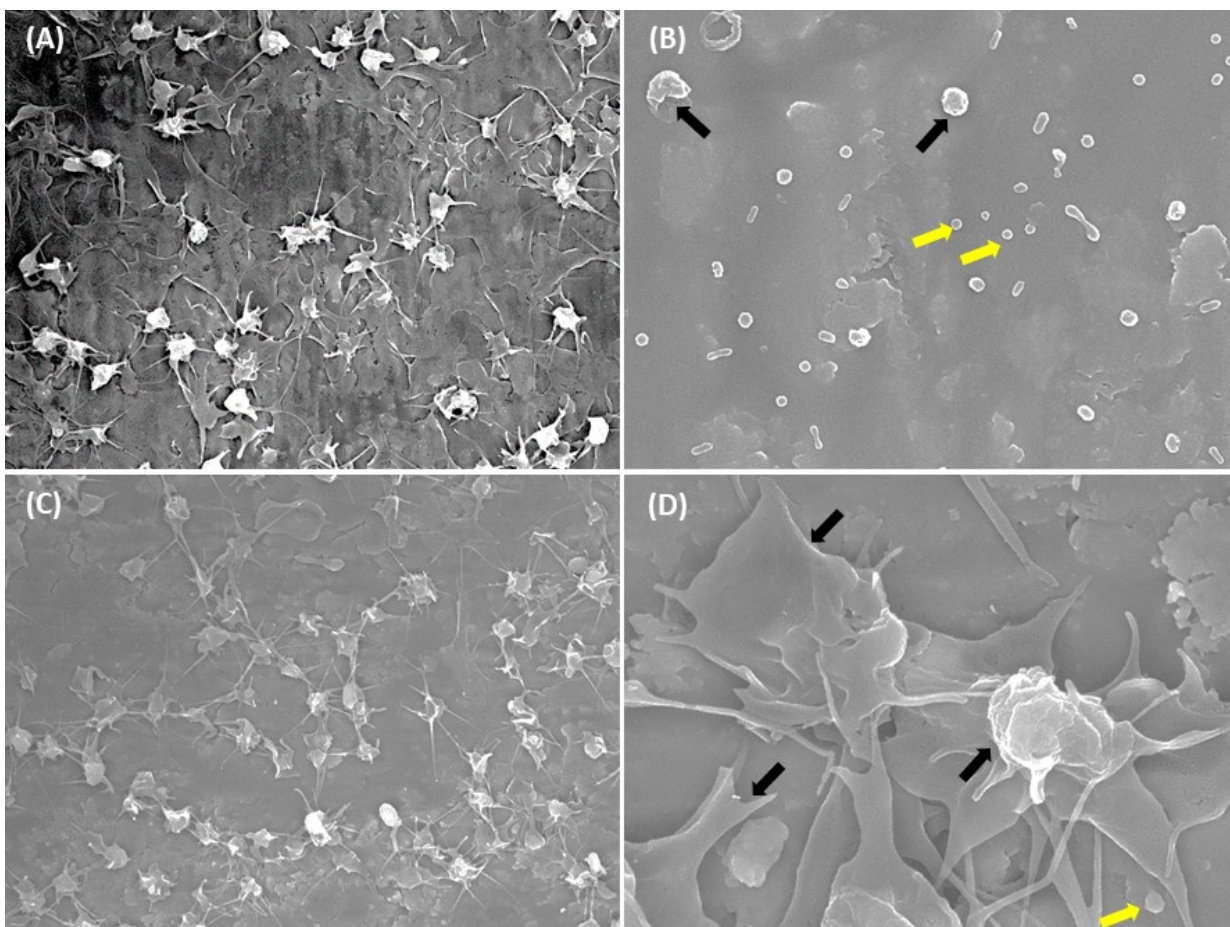


Figure 2. SEM of platelets and extracellular particles on A: untreated titanium foil (Ti foil), B: Ti foil+ PRP; C,D: Ti foil +PRP+EV. Yellow arrows indicate extracellular particles and black arrows indicate platelets at 3000 and 20000 magnifications respectively.

Figure 3 shows samples containing platelets and extracellular particles on microflowered Ti foil (Flowers_TiO₂) as imaged with SEM. It can be seen that only individual dendritic platelets existed (indicated by black arrows in Figure 3B and 3D). Furthermore, it can be difficult to observe vesicles on the surface. This could be due to the microstructuring of the surface due to roughened surface topography.

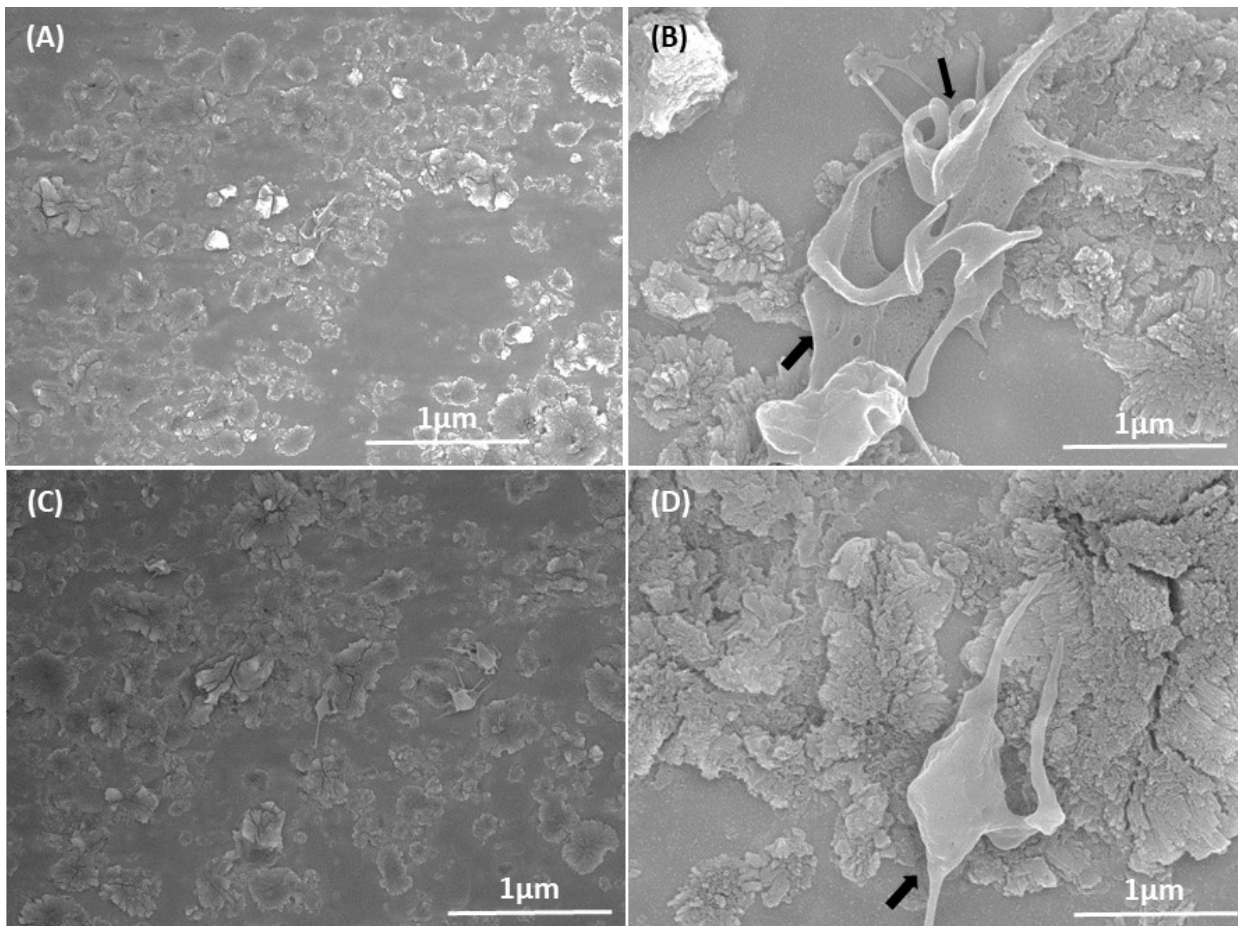


Figure 3. SEM of platelets and EVs on microflowered titanium surface (flowers_TiO₂): A, B: Flowers_TiO₂+PRP; C,D: Flowers_TiO₂+PRP+EV. Yellow arrows indicate EVs and black arrows indicate platelets at 3000 and 20000 magnifications respectively.

Figures 4 and **5** show samples containing platelets and EVs on plasma treated titanium surface (P_TiO₂) as imaged with SEM. It can be seen that the platelets (indicated by black arrows in Figure 4B and 4D) are highly activated exhibiting tubular protrusions. In Figure 4A and 4B numerous dendritic and extended platelets along with occasional vesicles can be observed whereas in case of P_TiO₂_PRP+EV no dendritic platelets were observed.

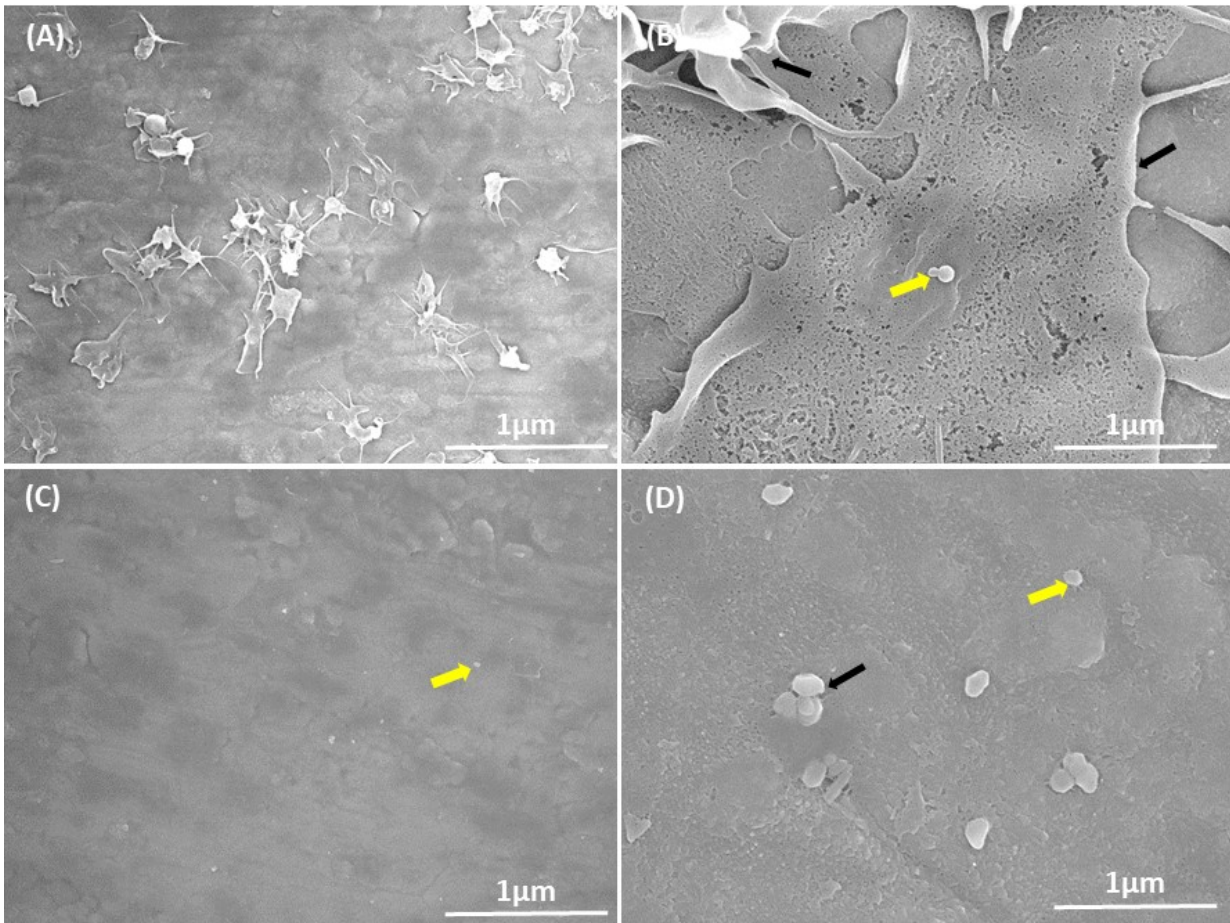


Figure 4. SEM of platelets and EVs on plasma treated titanium surface (P_TiO₂): A, B: P_TiO₂+ PRP; C,D: P_TiO₂+PRP+EV. Yellow arrows indicate extracellular particles and black arrows indicate platelets at 3000 and 20000 magnifications respectively.

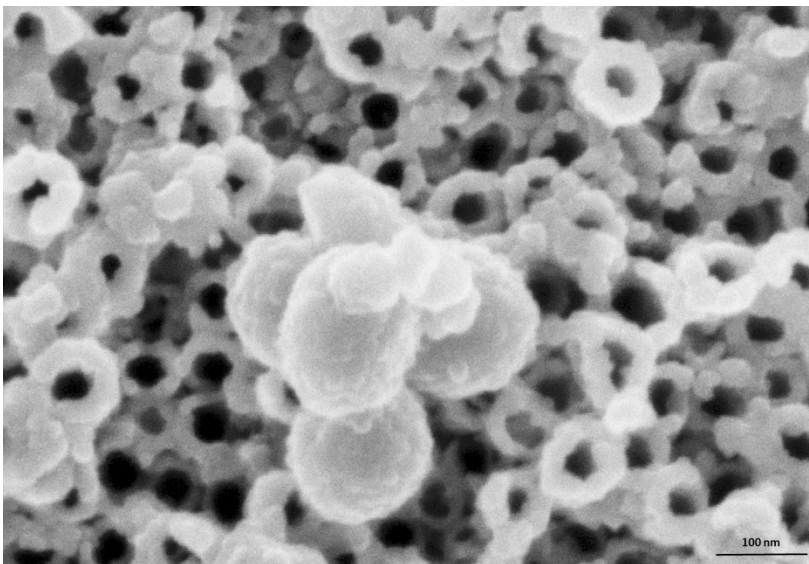


Figure 5. Scanning electron micrograph of EVs on TiO₂ nanotubes.



4. Conclusion

In present study we investigated the effect of different titanium surface treatments on the count and characteristics of platelets and EVs using FCM and SEM. FCM results revealed that P2* particles (predominantly platelets) were significantly more abundant than Pa* particles (primarily EVs) across all samples, particularly after incubation and in the pellet post-centrifugation. Centrifugation reduced P2* particles and slightly increased Pa* particles, indicating potential platelet fragmentation. SEM analysis corroborated these findings, showing high platelet activation and fragmentation across various Ti surfaces. However, the microflowered TiO₂ surface showed fewer vesicles, possibly due to its rougher topography. The study concluded that surface structuring of TiO₂ did not significantly affect particle counts, though mica effectively fragmented platelets. Overall, the SEM analysis provided more reliable detection of EVs, highlighting the need for further investigation into surface interactions and the limitations of FCM in this context.

Conflicts of Interest: The author declares no conflict of interest.

Acknowledgements. We would like to thank the Slovenian Research Agency (ARIS) for its financial support within grants P2-0232, J2-4447, J3-3074, J3-3066 and J3-2533.

References

- Božič D, Vozel D, Hočvar M, et al. Enrichment of plasma in platelets and extracellular vesicles by the counterflow to erythrocyte settling. *Platelets*. 2022; 33:592-602. DOI:10.1080/09537104.2021.1961716
- Castro-Giner F, Gkoutela S, Donato C, et al. Cancer Diagnosis Using a Liquid Biopsy: Challenges and Expectations. *Diagnostics (Basel)*. 2018; 8:31. DOI:10.3390/diagnostics8020031
- Cordonnier M, Chanteloup G, Isambert N, et al. Exosomes in cancer theranostic: Diamonds in the rough. *Cell Adh Migr*. 2017; 11:151-163. DOI:10.1080/19336918.2016.1250999
- Dong X, Chi J, Zheng L, Ma B, Li Z, et al. Efficient isolation and sensitive quantification of extracellular vesicles based on an integrated ExoID-Chip using photonic crystals. *Lab on a Chip*. 2019; 19:2897-2904. DOI:10.1039/C9LC00445A
- Fan GC, Han L, Zhu H, Zhang JR, Zhu JJ. Ultrasensitive photoelectrochemical immunoassay for matrix metalloproteinase-2 detection based on CdS:Mn/CdTe cosensitized TiO₂ nanotubes and signal amplification of SiO₂@Ab₂ conjugates. *Anal Chem*. 2014; 86:12398-12405. DOI:10.1021/ac504027d
- Golubnitschaja O, Flammer J. What are the biomarkers for glaucoma?. *Surv Ophthalmol*. 2007; 52:S155-S161. DOI:10.1016/j.survophthal.2007.08.011
- Jeran M, Romolo A, Spasovski V, et al. Small Cellular Particles from European Spruce Needle Homogenate. *Int J Mol Sci*. 2023; 24:4349. DOI:10.3390/ijms24054349
- Junkar I, Kulkarni M, Drašler B, et al. Influence of various sterilization procedures on TiO₂ nanotubes used for biomedical devices. *Bioelectrochemistry*. 2016; 109:79-86. DOI:10.1016/j.bioelechem.2016.02.001
- Junkar I, Kulkarni M, Drašler B, et al. Enhanced biocompatibility of TiO₂ surfaces by highly reactive plasma. *J. Phys. D: Appl. Phys*. 2016a; 49:244002. DOI:10.1088/0022-3727/49/24/244002
- Kralj-Iglič V. Membrane microvesiculation and its suppression. In *Advances in Planar Lipid Bilayers and Liposomes*. 2015; Chapter Six. pp. 177-204. <https://doi.org/10.1016/bs.adplan.2015.06.003>
- Kulkarni M, Mazare A, Gongadze E, et al. Titanium nanostructures for biomedical applications. *Nanotechnology*. 2015; 26:062002. DOI:10.1088/0957-4484/26/6/062002
- Li X, Corbett AL, Taatizadeh E, et al. Challenges and opportunities in exosome research-Perspectives from biology, engineering, and cancer therapy. *APL Bioeng*. 2019; 3:011503. DOI:10.1063/1.5087122
- Lim CZJ, Zhang L, Zhang Y, Sundah NR, Shao H. New Sensors for Extracellular Vesicles: Insights on Constituent and Associated Biomarkers. *ACS Sens*. 2020; 5:4-12. DOI:10.1021/acssensors.9b02165
- Martín-Gracia B, Martín-Barreiro A, Cuestas-Ayllón C, et al. Nanoparticle-based biosensors for detection of extracellular vesicles in liquid biopsies. *J Mater Chem B*. 2020; 8:6710-6738. DOI:10.1039/d0tb00861c
- Mavrič T, Benčina M, Imani R, et al. Electrochemical Biosensor Based on TiO₂ Nanomaterials for Cancer Diagnostics. *Advances in Biomembranes and Lipid Self-Assembly*. Academic Press. 2018; pp 63-105. <https://doi.org/10.1016/bs.abl.2017.12.003>



16. Mittal S, Kaur H, Gautam N, Mantha AK. Biosensors for breast cancer diagnosis: A review of bioreceptors, biotransducers and signal amplification strategies. *Biosens Bioelectron.* 2017; 88:217-231. DOI:10.1016/j.bios.2016.08.028
17. Popat KC, Eltgroth M, LaTempa TJ, Grimes CA, Desai TA. Titania nanotubes: a novel platform for drug-eluting coatings for medical implants?. *Small.* 2007; 3:1878-1881. DOI:10.1002/sml.200700412
18. Romolo A, Jan Z, Bedina Zavec A, et al. Assessment of Small Cellular Particles from Four Different Natural Sources and Liposomes by Interferometric Light Microscopy. *Int J Mol Sci.* 2022; 23:15801. DOI:10.3390/ijms232415801
19. Solanki PR, Kaushik A, Agrawal VV, Malhotra BD. Nanostructured metal oxide-based biosensors. *NPG Asia Materials.* 2011; 3:17-24. <https://doi.org/10.1038/asiamat.2010.137>
20. Strimbu K, Tavel JA. What are biomarkers?. *Curr Opin HIV AIDS.* 2010; 5:463-466. DOI:10.1097/COH.0b013e32833ed177
21. Turner APF. Biosensors: sense and sensibility. *Chem. Soc. Rev.* 2013; 42:3184-3196. <http://dx.doi.org/10.1039/C3CS35528D>
22. Vadlamani BS, Uppal T, Verma SC, Misra M. Functionalized TiO₂ Nanotube-Based Electrochemical Biosensor for Rapid Detection of SARS-CoV-2. *Sensors (Basel).* 2020; 20:5871. DOI:10.3390/s20205871
23. Wulfskuhle JD, Liotta LA, Petricoin EF. Proteomic applications for the early detection of cancer. *Nat Rev Cancer.* 2003; 3:267-275. DOI:10.1038/nrc1043
24. Xiao P, Zhang Y, Cao G. Effect of surface defects on biosensing properties of TiO₂ nanotube arrays. *Sensors and Actuators B: Chemical.* 2011; 155:159-164. DOI: 10.1016/j.snb.2010.11.041
25. Zhang H, Wang C, Chen B, Wang X. Daunorubicin-TiO₂ nanocomposites as a "smart" pH-responsive drug delivery system. *International journal of nanomedicine.* 2012; 7:235-242. DOI:10.2147/IJN.S27722
26. Zhang Y, Liu Y, Liu H, Tang WH. Exosomes: biogenesis, biologic function and clinical potential. *Cell Biosci.* 2019; 9:19. DOI:10.1186/s13578-019-0282-2